2013 IEEE/RSJ International Conference on
Intelligent Robots and Systems (IROS)
November 3-7, 2013. Tokyo, Japan

Single Beacon based Localization of AUVs using Moving Horizon Estimation

Sen Wang, Ling Chen, Huosheng Hu and Dongbing Gu

Abstract— **This paper studies the underwater localization problem for a school of robotic fish, i.e., a kind of Autonomous Underwater Vehicles with limited size, power and payload. These robotic fish cannot be equipped with traditional underwater localization sensors that are big and heavy. The proposed localization system is performed by using a single surface mobile beacon which provides range measurement to bound the localization error. The main contribution of this paper lies in twofold: 1) Observability of single beacon based localization is first analyzed in the context of nonlinear discrete time system, deriving a sufficient condition on observability. 2) Moving Horizon Estimation is then integrated with Extended Kalman Filters for three-dimensional localization using single beacon, which can reduce the computational complexity, impose various constraints and make use of previous range measurements for current estimation. Extensive numerical simulations are conducted to verify the observability and high localization accuracy of the proposed underwater localization method.**

I. Introduction

Recently, small and simple AUVs are increasingly adopted in many real-world applications in order to reduce costs and simplify design complexity. Their localization problem is acknowledged as an essential capability of these AUVs and has attracted an enormous attention [1]. Traditional underwater localization techniques, such as dead-reckoning and acoustic baseline systems, suffer from unbounded localization errors, expensive setting up, restricted operating area, etc. Therefore, some new underwater localization schemes have been proposed to overcome these drawbacks based on single mobile surface beacon and acoustic ranging technique [2]–[5].

In a single beacon based localization system, AUVs rely on range measurements from a surface vehicle to bound errors accumulated by dead-reckoning. Specifically, in [5] and [6], the centralized Extended Kalman Filter (EKF) and the decentralized Extended Information Filter (EIF) are proposed for both off-line and real-time localizations of AUVs equipped with highly accurate sensors, such as Doppler Velocity Log (DVL). In [2] and [3], three approaches based on EKF, Particle Filter (PF) and Non-linear Least Squares optimization (NLS) are proposed to perform cooperative localization in the absence of DVL. The NLS method has best performance yet increased computational complexity as all the previous calculated states and observed measurements are involved in the optimization. In [7], Wang *et al.* develop a finite-horizon H_∞ filtering for on-line robot localization without increasing the problem size over time. However, none of these methods considers constraints of state variable and process uncertainty. In [8] and [9], Moving Horizon Estimation (MHE), i.e. a Maximum a Posteriori (MAP) method, is used to formulate the robot localization problem into a fixed window optimization incorporating constraints. MHE is designed for two-dimensional localization problem with the aid of several static beacons or landmarks.

Since only range measurements from a single mobile beacon are used in our method to bound localization error of a group of AUVs, observability which determines the robot localizability should be investigated first. In [10]–[12], the rank of an observability matrix is used for observability analysis of linear systems or linearized nonlinear systems. But the original localization systems are usually non-linear and the linearization may cause wrong decision to observability [3]. Therefore, observability rank condition derived from Lie derivative for a nonlinear continuous time system is used in [3], [13], [14] to study the observability of robot localization. However, all these studies transform discrete time systems into continuous time systems for observability analysis under the assumption that the sample time is small enough, and no research has considered the observability of robot localization using nonlinear discrete system directly. Actually, most of localization systems and popular modern robot control systems are discrete-time system. Consequently, it is worth analyzing the observability of localization in the context of its discrete representation.

To address the aforementioned problems, a novel underwater localization scheme is proposed in this paper to provide the real-time localization capability for a school of robotic fish. The main contribution of this paper lies in twofold: 1) A straightforward method which is able to directly analyze observability of the single beacon localization in discrete time systems is proposed. A sufficient condition for the observability is also derived. 2) A localization algorithm which combines EKF and MHE to perform underwater localization in real-time is developed, avoiding unbounded computation increase and considering physical constraints. To the best knowledge of the authors, the method proposed in this paper is the first implementation of MHE in the context of single beacon based three-dimensional localization, using inaccurate model and measurements suffering low bandwidth and high latency.

The rest of this paper is organized as follows. Section II outlines the research problem and analyzes the observability. In Section III, the proposed localization algorithm is described. Section IV presents simulation results to evaluate the performance of the proposed algorithm. Finally, the

The authors are with School of Computer Science and Electronic Engineering, University of Essex, Colchester, CO4 3SQ, United Kingdom {swangi,lcheno,hhu,dgu}@essex.ac.uk

conclusion and future work are presented in Section V.

II. Localization with a Single Beacon

A. Problem Description

In this localization system, there are a school of robotic fish (RF) and a single beacon [15]. Each RF is equipped with a low-cost pressure sensor, an Inertial Measurement Unit (IMU) and an acoustic modem. Whereas, for the single beacon, the Global Positioning System (GPS) or some powerful and precise sensors are installed to make sure the reference position can be provided for the submerged RF. The RF can measure the ranges to the surface beacon by acoustic modem.

1) Kinematic Model: Because the underwater RF can neither access its velocities directly like mobile robots using odometry or AUVs with DVL nor can be modeled as accurate as its counterparts driven by propeller, the kinematic model of AUVs used in [5] is adopted and slightly changed in this paper. Consider position $\boldsymbol{s}_k$ and attitude $\boldsymbol{\varphi}_k$ (roll, pitch and yaw) of RF in the global coordinate frame as state $\boldsymbol{x}_k = [\boldsymbol{s}_k^T, \boldsymbol{\varphi}_k^T]^T$ to be estimated at time k, where $\boldsymbol{s}_k = [x_k, y_k, z_k]^T$ and $\boldsymbol{\varphi}_k = [\phi_k, \theta_k, \psi_k]^T$. The control input is $\boldsymbol{u}_k = [\boldsymbol{v}_k^T, \boldsymbol{\omega}_k^T]^T$ where $\boldsymbol{v}_k = [u_k, \nu_k, w_k]^T$ and $\boldsymbol{\omega}_k = [p_k, q_k, r_k]^T$ are the body-frame linear and angular velocities of RF respectively. Then, under the assumption that sampling time interval is Δ_T, the process model for RF can be represented as:

$$\boldsymbol{x}_{k+1} = f(\boldsymbol{x}_k, \boldsymbol{u}_k) = \boldsymbol{x}_k + \Delta_T J(\boldsymbol{x}_k)\boldsymbol{u}_k \tag{1}$$

where

$$J(\boldsymbol{x}) = \begin{bmatrix} \left[\boldsymbol{a}^1_{1\times3}{}^T \ \boldsymbol{a}^2_{1\times3}{}^T \ \boldsymbol{a}^3_{1\times3}{}^T\right]^T & \boldsymbol{0}_{3\times3} \\ \boldsymbol{0}_{3\times3} & \left[\boldsymbol{b}^1_{1\times3}{}^T \ \boldsymbol{b}^2_{1\times3}{}^T \ \boldsymbol{b}^3_{1\times3}{}^T\right]^T \end{bmatrix}$$

$$= \begin{bmatrix} c\psi c\theta & c\psi s\theta s\phi - s\psi c\phi & c\psi s\theta c\phi + s\psi s\phi & 0 & 0 & 0 \\ s\psi c\theta & s\phi s\psi s\theta + c\psi c\phi & s\psi s\theta c\phi - s\phi c\psi & 0 & 0 & 0 \\ -s\theta & c\theta s\phi & c\theta c\phi & 0 & 0 & 0 \\ 0 & 0 & 0 & 1 & s\phi t\theta & c\phi t\theta \\ 0 & 0 & 0 & 0 & c\phi & -s\phi \\ 0 & 0 & 0 & 0 & s\phi/c\theta & c\phi/c\theta \end{bmatrix}$$

is the transformation matrix and $\boldsymbol{0}$ denotes the zero matrix of compatible dimensions. Since $\boldsymbol{u}_k$ cannot be perceived in the absence of DVL, it is set to be constant herein. However, it is still assumed to be affected by an additive Gaussian noise $\boldsymbol{w}_k \sim \mathcal{N}(0, \boldsymbol{Q})$.

2) Measurement Models: The system model (1) cannot provide accurate movement prediction due to the random characteristics of control input $\boldsymbol{u}_k$. Therefore, the on-board IMU and pressure sensor are employed to refine the predicted attitude and depth of RF. However, the error of dead-reckoning increases unboundedly over time. Then, a single beacon is introduced to reduce the uncertainty and error of the localization by providing acoustic range measurement. The position of mobile beacon can be directly provided by GPS when surfacing, or estimated by SLAM when submerged [16]. This scheme where no expensive equipment is deployed on the RF can substantially reduce the hardware and energy cost of the whole system, especially for a shoal with enormous RF. The measurement model of RF with three types of measurements (range z_r, attitude $\boldsymbol{z}_a$ and depth z_d) is

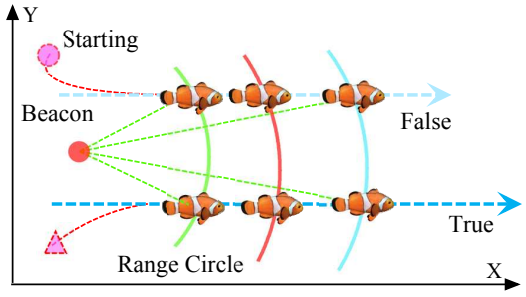

Fig. 1. Drawback of local observability using single static beacon.

$$\boldsymbol{z}_k = h(\boldsymbol{x}_k) + \boldsymbol{\mu}_k = \begin{bmatrix} z_{r,k} & \boldsymbol{z}_{a,k}^T & z_{d,k} \end{bmatrix}^T \tag{2}$$

where $\boldsymbol{\mu}_k \sim \mathcal{N}(0, \boldsymbol{R})$ is Gaussian noise. The details of these three measurements are below:

a) Range measurement: The single beacon broadcasts its position periodically via an acoustic modem for the RF to estimate the range by means of Time of Arrival. Denote the position of single beacon at time k as (x_k^b, y_k^b, z_k^b). Then, the range measurement is

$$z_{r,k} = \sqrt{(x_k^b - x_k)^2 + (y_k^b - y_k)^2 + (z_k^b - z_k)^2} + \mu_{r,k}. \tag{3}$$

We denote $\boldsymbol{H}_{r,k}$ as the Jacobian matrix of this equation with respect to $\boldsymbol{x}$, and R_r as the variance of range measurement.

b) Attitude measurement: The IMU measurement is used to estimate the attitude by

$$\boldsymbol{z}_{a,k} = \boldsymbol{H}_{a,k}\boldsymbol{x}_k + \boldsymbol{\mu}_{a,k} = \begin{bmatrix} \boldsymbol{0}_{3\times3} & \boldsymbol{I}_{3\times3} \end{bmatrix} \boldsymbol{x}_k + \boldsymbol{\mu}_{a,k} \tag{4}$$

where $\boldsymbol{I}$ denotes the identity matrix of compatible dimensions. The covariance of IMU measurement is $\boldsymbol{R}_a$.

c) Depth measurement: The depth measured by pressure sensor is related to the vertical position of RF. Then, the depth is

$$z_{d,k} = \boldsymbol{H}_{d,k}\boldsymbol{x}_k + \mu_{d,k} = \begin{bmatrix} 0 & 0 & 1 & \boldsymbol{0}_{1\times3} \end{bmatrix} \boldsymbol{x}_k + \mu_{d,k} \tag{5}$$

with the variance R_d.

The single beacon based multi-RF localization problem is how to simultaneously and accurately localize several RFs modeled as (1) with the aid of the measurement model (2). Because this system is nonlinear and discrete-time, the inherent nonlinear and discrete features are considered in the subsequent observability analysis and MHE based localization method.

B. Observability Analysis

Observability which is related to localizability in the context of robot localization is a necessary but not sufficient condition. Therefore, to successfully localize the robot, all the states have to be observable with respect to the measurement model. Observability analysis of nonlinear system is analyzed in this subsection since that of linearized system may result in wrong decision [3].

The criteria based on codistributions for observability of nonlinear discrete time system [17] is adopted to analyze the

observability and derive sufficient condition of this single beacon based localization. Consider the observation space $\boldsymbol{\Theta} = \bigcup_{k\geq 1} \boldsymbol{\Theta}_k$ constructed by the set of functions

$$\begin{aligned} \boldsymbol{\Theta_1} &= \{h\} \\ \boldsymbol{\Theta_k} &= \{h \circ f_{u_1} \circ \cdots \circ f_{u_j}, 1 \leq j \leq k-1\}, k \geq 2 \end{aligned} \tag{6}$$

where $f_u(x) = f(x,u)$ and $\circ$ denotes the function composition, i.e., $g \circ f(x) = g(f(x))$. According to the criteria in [17], nonlinear discrete time system is locally weakly observable if $\dim d\boldsymbol{\Theta} = n$ where $d\boldsymbol{\Theta}$ is the differential of space $\boldsymbol{\Theta}$ and n is the system order.

For the system described above, the number of system state variables to be tested is 6. According to (2) and (6), it yields

$$\boldsymbol{\Theta_1} = \begin{bmatrix} \underbrace{h_{r1}}_{z_r} & \underbrace{\phi \quad \theta \quad \psi}_{\boldsymbol{z}_a} & \underbrace{z}_{z_d} \end{bmatrix}^T \tag{7}$$

where $h_{r1} = \sqrt{(x^b - x)^2 + (y^b - y)^2 + (z^b - z)^2}$. Then, the gradient of the measurement with respect to the system state $\boldsymbol{x}$ is

$$\nabla\boldsymbol{\Theta_1} = \begin{bmatrix} \frac{x^b - x}{h_{r1}} & \frac{y^b - y}{h_{r1}} & \frac{z^b - z}{h_{r1}} & 0 & 0 & 0 \\ 0 & 0 & 0 & 1 & 0 & 0 \\ 0 & 0 & 0 & 0 & 1 & 0 \\ 0 & 0 & 0 & 0 & 0 & 1 \\ 0 & 0 & 1 & 0 & 0 & 0 \end{bmatrix} \tag{8}$$

It can be seen that the minimum rank of $\nabla\boldsymbol{\Theta_1}$ is 4. In order to guarantee the local observability of the system by keeping the full rank of $d\boldsymbol{\Theta}$, the first two columns of $\nabla\boldsymbol{\Theta}$ should be independent of each other. The composition $\boldsymbol{\Theta_2} = h \circ f$ is

$$\boldsymbol{\Theta_2} = \begin{bmatrix} h_{r2} & \phi + \Delta B_1 & \theta + \Delta B_2 & \psi + \Delta B_3 & s_3 \end{bmatrix}^T \tag{9}$$

where

$$\begin{aligned} h_{r2} &= \sqrt{(x^b - s_1)^2 + (y^b - s_2)^2 + (z^b - s_3)^2} \\ s_1 &= x + \Delta_T \boldsymbol{a}^1 \boldsymbol{v}, s_2 = y + \Delta_T \boldsymbol{a}^2 \boldsymbol{v}, s_3 = z + \Delta_T \boldsymbol{a}^3 \boldsymbol{v} \\ \Delta B_i &= \Delta_T \boldsymbol{b}^i \boldsymbol{\omega}, i = 1, 2, 3. \end{aligned}$$

Therefore, by calculating the gradient of $\boldsymbol{\Theta_2}$, we have

$$\nabla\boldsymbol{\Theta_2} = \begin{bmatrix} \frac{x^b - s_1}{h_{r2}} & \frac{y^b - s_2}{h_{r2}} & * & * & * & * \\ 0 & 0 & * & * & * & * \\ 0 & 0 & * & * & * & * \\ 0 & 0 & * & * & * & * \\ 0 & 0 & * & * & * & * \end{bmatrix} \tag{10}$$

where $*$ are the equations whose specifics are ignored for clarity. Consequently, from (8) and (10), an observability submatrix formed by extracting the first two columns is

$$\mathcal{O} = \begin{bmatrix} \frac{x^b - x}{h_{r1}} & \frac{y^b - y}{h_{r1}} \\ \frac{x^b - x - \Delta_T \boldsymbol{a}^1 \boldsymbol{v}}{h_{r2}} & \frac{y^b - y - \Delta_T \boldsymbol{a}^2 \boldsymbol{v}}{h_{r2}} \end{bmatrix} \tag{11}$$

In order to satisfy $\dim d\boldsymbol{\Theta} = n$, the determinant of $\mathcal{O}$ must be nonzero. Under the assumption that the measured range cannot be zero, i.e., $h_r \neq 0$, the sufficient condition for observability is

$$(y^b - y)\Delta_T \boldsymbol{a}^1 \boldsymbol{v} - (x^b - x)\Delta_T \boldsymbol{a}^2 \boldsymbol{v} \neq 0. \tag{12}$$

Because $\boldsymbol{a}^1$ and $\boldsymbol{a}^2$ in (1) are related to $\boldsymbol{\varphi}$, the observability of the system is determined by $\boldsymbol{\varphi}$, $\boldsymbol{v}$ and the relative position between the beacon and the RF. Since the sufficient condition (12) can only ensure local observability rather than global one, some trajectories of RF and beacon are not distinguishable using a single static beacon as shown in Fig. 1. A solution is to design appropriate path planning [18], improving the observability. The observability analysis verifies that the measurement (2) is sufficient for localization.

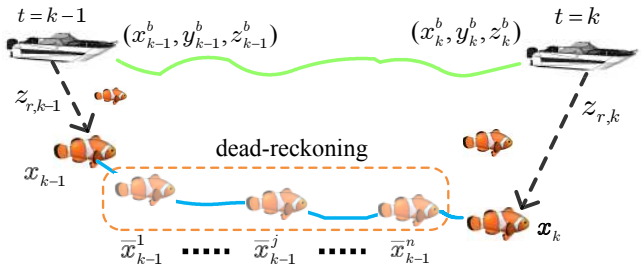

Fig. 2. System description between two steps.

C. State Constraints

Some available prior knowledge of system and environment can be applied to constrain the state variables and noises. The constraints usually exist in the form of equality or inequality. Suppose the state variables, control inputs and disturbances satisfy the following q constraints:

$$g_i(\boldsymbol{x}, \boldsymbol{u}, \boldsymbol{w}) \leq 0, \qquad i = 1, \cdots, q. \tag{13}$$

When performing the state estimation, these constraints which can be accessed from the prior knowledge or geometry of the environment should be taken into account to make sure the results are reasonable and accurate.

III. EKF and MHE based Localization Algorithm

With the system model described above, attitude, depth and range measurement could be fused together to perform localization. However, since attitude and depth data from IMU and pressure sensors is obtained rapidly and range measurements are updated at a low rate, several filters are utilized to fuse data asynchronously. Specifically, EKF is used to update the prediction using attitude and depth measurements, which serves as dead-reckoning. Once a range observation is available, current position is ameliorated by MHE, which can not only restrain the noise and smooth the estimate but also consider constraints on the operating environment and physical system. The reason for why both EKF and MHE are employed lies in that the real-time feature of EKF is suitable for high frequency update (attitude and depth) while MHE incorporates several previous range measurements at one estimation, compensating for single range measurement.

A. Prediction and Update using Attitude and Depth

Prediction and update on attitude and depth comprise dead-reckoning. Traveled displacement and direction change with respect to the previous pose are estimated.

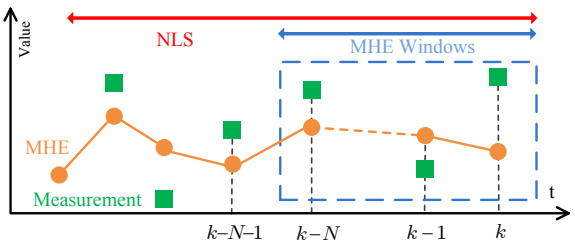

Fig. 3. MHE with fixed-size window.

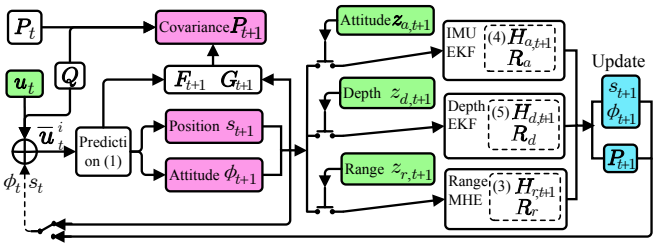

Fig. 4. Scheme of localization algorithm.

1) Prediction: The state $\boldsymbol{x}$ is propagated by using model (1), and the covariance matrix $\boldsymbol{P}$ at time k is obtained by

$$\boldsymbol{P}_k = \boldsymbol{F}_k \boldsymbol{P}_{k-1} \boldsymbol{F}_k^T + \boldsymbol{G}_k \boldsymbol{Q}_k \boldsymbol{G}_k^T \tag{14}$$

where $\boldsymbol{F}_k$ and $\boldsymbol{G}_k$ are the Jacobian matrices of (1) with respect to $\boldsymbol{x}_k$ and $\boldsymbol{w}_k$ respectively. This prediction is conducted using constant velocity due to the absence of DVL, which produces serious errors as time goes.

2) Update using Attitude and Depth Measurements: IMU and pressure sensor are introduced to reduce the error accumulation of the prediction. Because both measurements can be acquired much faster than range measurement, the prediction is updated by attitude and depth measurements at a high rate. Once an attitude or depth measurement is received, EKF is used to update their state and covariance using (4), (5) or (14) without noises. Technical detail of EKF design is omitted here due to its straightforward steps.

B. MHE based Update using Range Measurement

When a range measurement is received by RF, the current state propagated by dead-reckoning is updated by MHE. According to the observability analysis in Subsection II-B, update on x and y highly relies on this range observation.

Assuming the nosies are Gaussian, the NLS method proposed in [2] can be formed as the following optimization problem in the context of our system model:

$$\underset{\boldsymbol{x}_{0:k}}{\operatorname{argmin}} \sum_{t=0}^{k-1} \|\boldsymbol{w}_t\|^2_{\boldsymbol{Q}_{r,t}^{-1}} + \sum_{t=1}^{k} \|\mu_{r,t}\|^2_{R_r^{-1}} \tag{15}$$

where $\|z\|_A^2 := z^T A z$, and $\boldsymbol{Q}_{r,t}$ is covariance of the process noise at time t. Since the range measurements obtained from the beginning are all incorporated into this optimization problem to calculate the state set $\{\boldsymbol{x}_0^k\} = \{x_0, \cdots, x_k\}$, the number of the state variables and computational complexity increase over time.

MHE is adopted to overcome the drawbacks of NLS. Moreover, the constraints on state, control input, noise, etc. can be imposed to refine the localization results. Consider the MAP derivation and the MHE theory in [19]. The objective function $\Phi_k(\{\boldsymbol{x}_0^k\})$ of MHE which is similar to (15) can be represented by separating the time interval into two sections $\{t : 0 \le t \le k-N\}$ and $\{t : k-N+1 \le t \le k\}$:

$$\Phi_k(\{\boldsymbol{x}_0^k\}) = \sum_{t=k-N}^{k-1} \|\boldsymbol{w}_t\|^2_{\boldsymbol{Q}_{r,t}^{-1}} + \sum_{t=k-N+1}^{k} \|\mu_{r,t}\|^2_{R_r^{-1}} + \sum_{t=0}^{k-N-1} \|\boldsymbol{w}_t\|^2_{\boldsymbol{Q}_{r,t}^{-1}} + \sum_{t=1}^{k-N} \|\mu_{r,t}\|^2_{R_r^{-1}} + \|\boldsymbol{x}_0 - \hat{\boldsymbol{x}}_0\|^2_{\boldsymbol{Q}_{r,0}^{-1}}$$

where N is the size of estimation window and $\hat{\boldsymbol{x}}_0$ is the initial position. Since the shadowed part only relies on the states $\{\boldsymbol{x}_{k-N}^k\}$ and the range measurements $\{z_{r,k-N+1}^k\}$, the optimization can be transformed into a problem with fixed-window size, as shown in Fig. 3, by approximating the rest part of the objective function to an arrival cost. By denoting the set $\{\boldsymbol{w}_{k-N}^{k-1}\}$ as the input disturbances from time $k-N$ to time $k-1$, the states of interest can be calculated by process model (1). Therefore, the MHE at time k considering the constraints (13) is

$$\begin{aligned} \underset{\boldsymbol{x}_{T_s}, \{\boldsymbol{w}_{T_s}^{k-1}\}}{\operatorname{argmin}} \quad & \sum_{t=T_s}^{k-1} \|\boldsymbol{w}_t\|^2_{\boldsymbol{Q}_{r,t}^{-1}} + \sum_{t=T_s+1}^{k} \|\mu_{r,t}\|^2_{R_r^{-1}} + \mathcal{Z}_{T_s}(\boldsymbol{x}_{T_s}) \\ \text{s.t.} \quad & g_i(\boldsymbol{x}, \boldsymbol{u}, \boldsymbol{w}) \le 0, \qquad i = 1, \cdots, q \end{aligned} \tag{16}$$

where $T_s = k - N$ is the starting time of MHE window, and $\mathcal{Z}_{T_s}$ is the approximation of arrival cost at time T_s. The arrival cost $\mathcal{Z}_{T_s}$ is essential in the MHE because it bounds the original optimization problem into fixed size. Then, the key is how to properly approximate the past data. By employing the EKF approximation in [19], the arrival cost is given by

$$\mathcal{Z}_{T_s}(\boldsymbol{x}_{T_s}) = \|\boldsymbol{x}_{T_s} - \hat{\boldsymbol{x}}_{T_s}\|^2_{\boldsymbol{P}_{T_s}^{-1}} \tag{17}$$

where the covariance $\boldsymbol{P}$ is propagated by

$$\begin{aligned} \boldsymbol{P}_{k+1} = \boldsymbol{G}_k \boldsymbol{Q}_k \boldsymbol{G}_k^T + \\ \boldsymbol{F}_k (\boldsymbol{P}_k - \boldsymbol{P}_k \boldsymbol{H}_{r,k}^T (R_r + \boldsymbol{H}_{r,k} \boldsymbol{P}_k \boldsymbol{H}_{r,k}^T)^{-1} \boldsymbol{H}_{r,k} \boldsymbol{P}_k) \boldsymbol{F}_k^T. \end{aligned}$$

The current estimate $\hat{\boldsymbol{x}}_k$ can be yielded by substituting the obtained $\boldsymbol{x}_{T_s}$ and $\{\boldsymbol{w}_{T_s}^{k-1}\}$ and the set of control input $\{\boldsymbol{u}_{T_S}^{k-1}\}$ into (1) recursively. An intuitive idea to incorporate $\{\boldsymbol{u}_{T_S}^{k-1}\}$ is to augment the optimization variables by including the positions $\bar{\boldsymbol{x}}_i^j, i = T_s, \ldots, k-1$ maintained by dead-reckoning, see Fig. 2. However, this is extremely high computational complexity. Therefore, we employ the accumulation $\sum_{j=1}^{n} \bar{\boldsymbol{u}}_t^j$ between two consecutive range measurements t and $t+1$ as the approximate control input $\boldsymbol{u}_t$. The scheme of the designed whole localization method can be seen in Fig. 4.

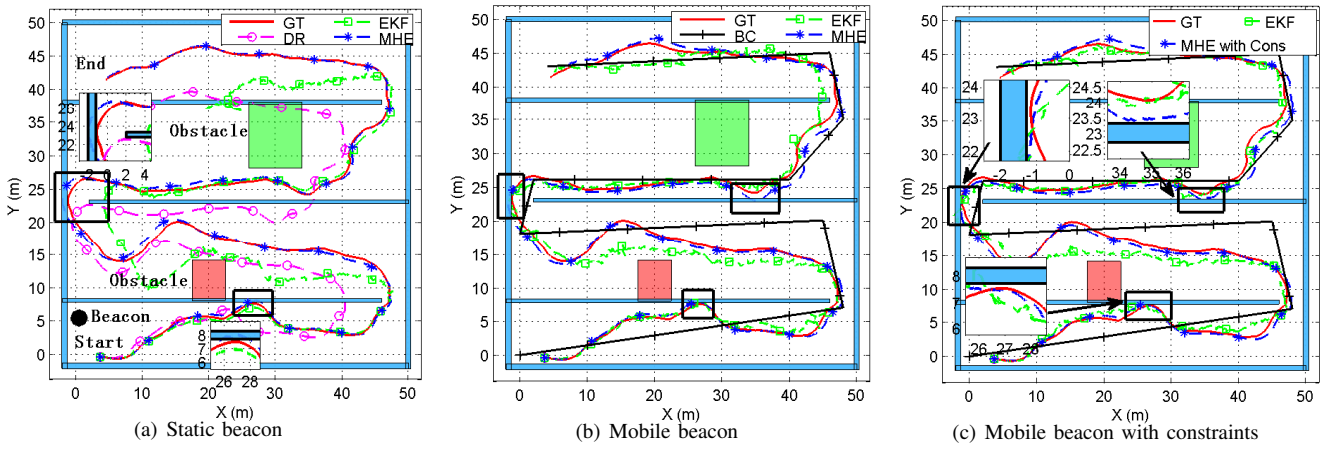

(a) Static beacon (b) Mobile beacon (c) Mobile beacon with constraints

Fig. 5. Localization trajectories of dead-reckoning, EKF and MHE with static or mobile surface beacons.

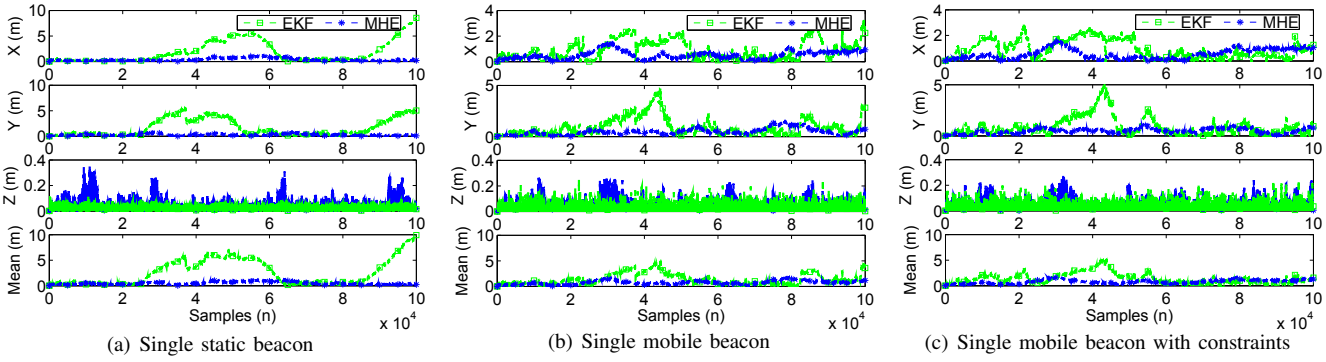

(a) Single static beacon (b) Single mobile beacon (c) Single mobile beacon with constraints

Fig. 6. Localization errors of dead-reckoning, EKF and MHE with single static or mobile surface beacon.

IV. Simulation Results

In this section, the performance of the proposed localization algorithm is evaluated through simulation. The simulated data is sampled by using Robot Operating System. For comparison, the localization trajectories and errors of the dead-reckoning, EKF and MHE in three different scenarios are presented. The $52m \times 52m \times 20m$ blue boundary in Fig. 5(a) shows the operating field with channel and obstacles. It takes about 20 minutes for the RF to travel the whole trip in simulation. According to the specification of Tritech micron acoustic modem, the range update frequency is set to be 1 Hz and $R_r = (0.2m)^2$. The frequencies of IMU and pressure sensor are both 100 Hz with $\boldsymbol{R}_a = (0.36\text{rad/s})^2 I$ and $R_d = (0.2m)^2$. Note that the localization algorithms are all fed with the same control input and observations.

Fig. 5 shows the ground truth of RF and the corresponding localization trajectories using dead-reckoning, EKF and MHE with the aid of the single static beacon, mobile beacon and mobile beacon with constraints. In Fig. 5(a), where a single static beacon is used, the dead-reckoning gradually diverges from the ground truth, which means the errors on x and y are accumulated. In contrast, the result of EKF which fuses the range measurements is accurate in certain periods with bounded errors although it is worse than that of the MHE (see Fig. 6(a)). The reason is that only single range observation is available for each step and the observability cannot be improved effectively. Since several previous range measurements are used in one estimation, the MHE method is able to converge to the ground truth with high accuracy. However, as shown in the enlargements in Fig. 5(a), the trajectory of MHE crosses the boundary occasionally, which is not reasonable in reality.

Using a single surface mobile beacon , the localization accuracy of EKF is improved as described in Fig. 5(b) and 6(b), which validates that the beacon mobility increases the observability. However, the performance of EKF in terms of localization accuracy is still inferior to MHE. Although the mobile beacon is employed, the problem of MHE that trajectory is beyond the boundary has not been solved yet. After introducing the boundary constraints into MHE, all the estimates are confined in the channel as can be seen from the magnified parts in Fig. 5(c). These numerical evaluations verify that the MHE method can produce more accurate localization estimation than EKF in the context of single beacon and it is more suitable for single beacon based localization.

The overall uncertainty of the position estimate in three dimension is proportional to the square root of the determinant of the covariance on x, y, z, i.e., $\sqrt{\det P_{x,y,z}}$. According to this relation, the spatial uncertainties of dead-reckoning, EKF and MHE methods in one trial are presented in Fig.

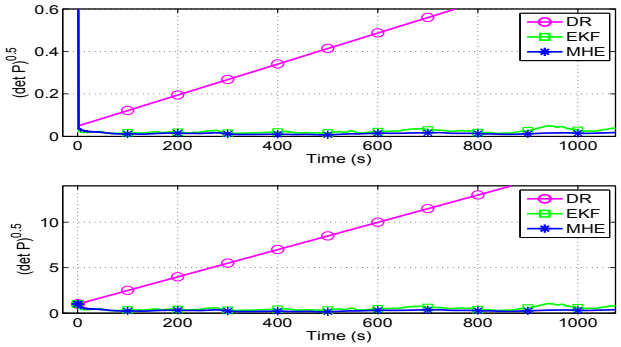

Fig. 7. Overall Uncertainty on position x, y, z and x, y only.

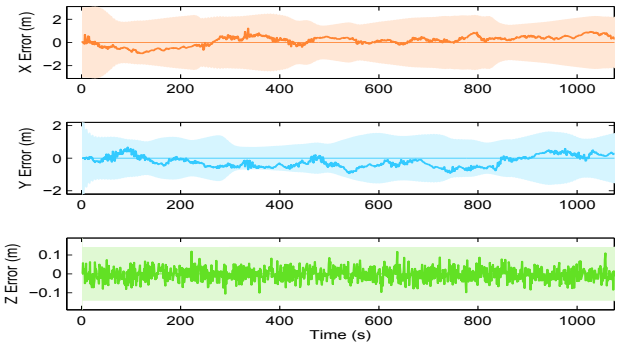

Fig. 8. Estimation errors on x, y, z and their 3σ confidence intervals.

7. As expected, the uncertainty of dead-reckoning grows monotonically without bound while these of EKF and MHE are not increased over time. The initial large uncertainties of EKF and MHE are also decreased and converged. The uncertainties of orientation of three methods are all bounded thanks to the IMU, which can be analyzed similarly.

Corresponding to Fig. 7, Fig. 8 shows the localization errors on x, y, z of MHE against their respective $\pm 3\sigma$ confidence intervals. All the errors are within their lower and upper confidence bounds with extra allowance, which indicates that the estimation of this MHE based localization is reliable and the proposed algorithm is effective.

V. Conclusions

This paper proposes a novel 3D underwater localization system with a single beacon, which combines EKF and MHE. It uses dead-reckoning and range measurements to provide accurate location with bounded errors for the small AUVs. The observability of single beacon based localization is analyzed in the context of a nonlinear discrete time system, producing the sufficient condition for single beacon based localization. Compared with EKF, the high localization accuracy and effectiveness of the proposed approach are validated by simulation in different scenarios. Our future work will focus on the implementation of the proposed method on real robotic fish in a lake or sea.

Acknowledgment

This research is financially supported by the research grant "Robotic fish for wider University engagement and market exploitation" funded by REO Development Fund at Essex University, FI03005. Our thanks also go to Robin Dowling for his technical support during the research.

References

[1] L. Chen, S. Wang, K. McDonald-Maier, and H. Hu, "Towards autonomous localization and mapping of AUVs: A survey," *Int. J. of Intelligent Unmanned Systems*, vol. 1, no. 2, pp. 97–120, 2013.

[2] G. Papadopoulos, M. F. Fallon, J. J. Leonard, and N. M. Patrikalakis, "Cooperative localization of marine vehicles using nonlinear state estimation," in *Proc. IEEE/RSJ Int. Conf. Intell. Robots Syst.* IEEE, Oct. 2010, pp. 4874–4879.

[3] M. F. Fallon, G. Papadopoulos, J. J. Leonard, and N. M. Patrikalakis, "Cooperative AUV navigation using a single maneuvering surface craft," *Int. J. Robot. Res.*, vol. 29, no. 12, pp. 1461–1474, 2010.

[4] S. Webster, R. Eustice, H. Singh, and L. Whitcomb, "Preliminary deep water results in single-beacon one-way-travel-time acoustic navigation for underwater vehicles," in *Proc. IEEE/RSJ Int. Conf. Intell. Robots Syst.* IEEE, 2009, pp. 2053–2060.

[5] S. E. Webster, R. M. Eustice, H. Singh, and L. L. Whitcomb, "Advances in single-beacon one-way-travel-time acoustic navigation for underwater vehicles," *Int. J. Robot. Res.*, vol. 31, no. 8, pp. 935–950, May 2012.

[6] S. E. Webster, L. L. Whitcomb, and R. M. Eustice, "Advances in decentralized single-beacon acoustic navigation for underwater vehicles: theory and simulation," in *2010 IEEE/OES Autonomous Underwater Vehicles*. IEEE, 2010, pp. 1–8.

[7] Z. Wang, H. Dong, B. Shen, and H. Gao, "Finite-horizon H-infinity filtering with missing measurements and quantization effects," *IEEE Trans. Automat. Contr.*, vol. 58, no. 7, pp. 1707–1718, 2013.

[8] A. Simonetto, D. Balzaretti, and T. Keviczky, "A distributed moving horizon estimator for mobile robot localization problems," in *World Congress*, vol. 18, no. 1, 2011, pp. 8902–8907.

[9] G. Pillonetto, A. Aravkin, and S. Carpin, "The unconstrained and inequality constrained moving horizon approach to robot localization," in *Proc. IEEE/RSJ Int. Conf. Intell. Robots Syst.* IEEE, 2010, pp. 3830–3835.

[10] A. Gadre and D. Stilwell, "A complete solution to underwater navigation in the presence of unknown currents based on range measurements from a single location," in *Proc. IEEE/RSJ Int. Conf. Intell. Robots Syst.* IEEE, 2005, pp. 1420–1425.

[11] A. Gadre, "Observability analysis in navigation systems with an underwater vehicle application," Ph.D. dissertation, Virginia Polytechnic Institute and State University, 2007.

[12] G. P. Huang, N. Trawny, A. I. Mourikis, and S. I. Roumeliotis, "Observability-based consistent EKF estimators for multi-robot cooperative localization," *Auton. Robots.*, vol. 30, no. 1, pp. 99–122, Sept. 2010.

[13] A. Martinelli and R. Siegwart, "Observability analysis for mobile robot localization," in *Proc. IEEE/RSJ Int. Conf. Intell. Robot. Syst.* IEEE, 2005, pp. 1471–1476.

[14] G. Antonelli, F. Arrichiello, S. Chiaverini, and G. S. Sukhatme, "Observability analysis of relative localization for AUVs based on ranging and depth measurements," in *Proc. IEEE Int. Conf. Robot. Autom.* IEEE, May 2010, pp. 4276–4281.

[15] S. Wang, L. Chen, H. Hu, Z. Xue, and W. Pan, "Underwater localization and environment mapping using wireless robots," *Wireless Pers. Commun.*, vol. 70, no. 3, pp. 1147–1170, 2013.

[16] D. Ribas, P. Ridao, J. Neira, and J. D. Tardos, "SLAM using an imaging sonar for partially structured underwater environments," in *Proc. IEEE/RSJ Int. Conf. Intell. Robots Syst.* IEEE, 2006, pp. 5040–5045.

[17] F. Albertini and D. D'Alessandro, "Observability and forward–backward observability of discrete-time nonlinear systems," *Math Control Signal*, vol. 15, no. 4, pp. 275–290, 2002.

[18] G. Antonelli, A. Caiti, V. Calabro, and S. Chiaverini, "Designing behaviors to improve observability for relative localization of AUVs," in *Proc. IEEE Int. Conf. Robot. Autom.* IEEE, 2010, pp. 4270–4275.

[19] C. Rao, J. Rawlings, and D. Mayne, "Constrained state estimation for nonlinear discrete-time systems: stability and moving horizon approximations," *IEEE Trans. Automat. Contr.*, vol. 48, no. 2, pp. 246–258, Feb. 2003.